JOURNAL OF AIRCRAFT
Vol. 36, No. 6, November–December 1999

Manual Aerodynamic Optimization of an Oblique Wing Supersonic Transport

Pei Li*
The Boeing Company, Seattle, Washington 98124
Helmut Sobieczky†
DLR, German Aerospace Center, D-37073 Göttingen, Germany
and
Richard Seebass‡
University of Colorado, Boulder, Colorado 80309

We use manual methods and an advanced geometry generator to optimize a large wing flying obliquely at $M_\infty = \sqrt{2}$. These include the informed, but manual, design of the airfoil sections and a blending of these airfoil sections to create the wing. A manual tailoring of the wing planform and planform (twist axis) bending are used to ensure a nearly elliptic load. The lift coefficient and sweep are varied sequentially to arrive at an optimum inviscid design. The viscous drag is estimated by considering the wing to be a flat plate. The altitude at which the wing enters cruise is selected to maximize *L/D*. This results in an oblique wing supersonic transport that reaches Mach 0.8 at 30,800 ft, where it has a viscous *ML/D* of 24.9, accelerates through Mach 1.1, where it has a viscous *ML/D* of 23.7, to cruise at Mach $\sqrt{2}$ at 41,300 ft. There its viscous *ML/D* is 24.2.

Special Dedication

This paper is dedicated to R. T. Jones to honor his contributions to diverse fields, but most especially his contributions to our understanding of supersonic aerodynamics.

Introduction

NEARLY 50 years ago R. T. Jones[1,2] noted that an oblique elliptic wing has the minimum inviscid drag due to lift. As suggested in the following, this result is more easily derived using Lomax's interpretation of the area rule given by Hayes,[3] Lomax,[4] and Lomax and Heaslet.[5] A decade later Smith[6] noted that the Sears–Haack area distribution is the product of an elliptic and a parabolic distribution. This means that an elliptic wing with an elliptic load and a parabolic thickness distribution will have the minimum drag due to lift and the minimum wave drag because of volume. Van der Velden[7,8] and others[9–13] have reminded us that a large wing flying obliquely warrants serious study both as a near sonic transport and as a supersonic transport. Because such an aircraft is efficient at both transonic and supersonic speeds, it can provide near sonic, or slightly supersonic, transport over land and supersonic transport over water, thereby providing much reduced travel times. The aircraft should be able to do so with aerodynamic and structural efficiencies that exceed those of future subsonic transports with bilateral symmetry. Such an aircraft is depicted in Fig. 1. Modern control and vectored-thrust technologies will probably result in the engines being internal to the wing and having no need for vertical stabilizers.

As a transport aircraft, the oblique wing's thickness is set by the need to provide aisles for the passengers. The chord of the wing is then set by the maximum thickness-to-chord ratios achievable for airfoils that will result in an efficient wing at the cruise Mach number. The wing's span and length are set by the aerodynamic efficiency required to compete with current subsonic transports. This means that an oblique wing supersonic transport must be a large aircraft.

We consider here the manual optimization of an 800 passenger oblique wing transport for a cruise Mach number of $\sqrt{2}$. This choice derives from the studies of Ref. 9. Although higher Mach numbers were considered in this study, they required sweep angles that seem impractical. Such a wing, as presented here, would take off with a sweep of 40 deg, and as it accelerated through sonic conditions to its cruise Mach number, would increase its sweep to 65 deg.

The low induced drag of an oblique wing derives from its considerable span (measured normal to the freestream). The low wave drag derives from the wing's considerable length and the ability to provide the optimum distribution of lift and volume in all oblique planes. The aerodynamic advantages of the oblique wing over a wing with bilateral symmetry stems solely from these facts. An elliptic wing swept behind the Mach cone will not naturally provide the elliptic load needed to minimize the induced drag and wave drag because of lift. The downwash will vary nearly linearly down the wing and bending, twist, and/or section thickness variation, must be used to achieve an elliptic load distribution. Because the section areas are fixed to minimize the wave drag because of volume (or caliber), bending and twist must be employed. Parabolic bending of the wing, as shown in Fig. 2, provides a linear twist whose magnitude is proportional to the sine of the sweep angle λ, providing an approximately elliptic load even as the wing's sweep is varied.

Supporting Theories

The theories that support the concept of an oblique wing transport comprise the area rule, minimum wave drag bodies of revolution, and supercritical or shock-free airfoil theory. The results provided here derive from these theories. That an oblique wing provides the minimum inviscid drag for a given lift was first derived by Jones[1,2] using the reverse-flow theory of Munk.[14] It can also be derived by considering the streamwise and downward momentum fluxes through the rear Mach fore cone.[15,16]

Received 15 December 1997; presented as Paper 98-0598 at the AIAA 36th Aerospace Sciences Meeting, Reno, NV, 12–15 January 1998; revision received 5 April 1999; accepted for publication 20 May 1999.

*Research Associate, P.O. Box 3707, Mail Stop 67-LF, NSF CISE, Aerospace Engineering Sciences, University of Colorado; currently Senior Specialist Engineer, Boeing Commercial Airplane Group. Member AIAA.

†Senior Research Scientist, Bunsenstrasse 10. Associate Fellow AIAA.

‡John R. Woodhull/Logicon Professor of Aerospace Engineering Sciences. Fellow AIAA.

Fig. 1 NASA artist's concept of R. T. Jones' oblique wing supersonic transport.

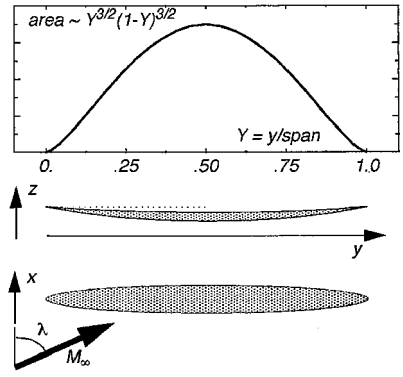

Fig. 2 Oblique wing swept at angle λ with an elliptic planform, parabolic bending, and a Sears–Haack area distribution.

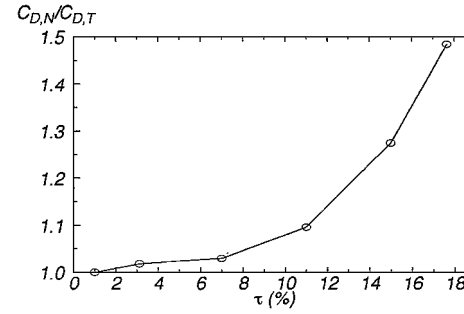

Fig. 3 Ratio of the inviscid nonlinear numerical drag coefficient to the corresponding linear theory values for the wing of Fig. 1 with $M_\infty = \sqrt{2}$ and $\lambda = 60$ deg.

Area Rule

The supersonic area rule as expressed by Lomax,[4] and Lomax and Heaslet[5] tells us that the wave drag of an aircraft in a steady supersonic flow is identical to the azimuthal average wave drag of an azimuthal series of equivalent bodies of revolution. For each azimuthal angle the cross-sectional area of the equivalent body of revolution is given by the sum of a volume and a lift contribution. The volume contribution is that due to a body of revolution whose cross-sectional area equals that of the cross section of the aircraft cut by the tangent to the fore Mach cone projected onto the plane perpendicular to the freestream. The lift contribution is that due to an area distribution that equals $2\beta/q$ times the component of force on the contour cut by the fore Mach cone that lies in the cut's azimuthal plane; this area is then projected onto the plane perpendicular to the freestream. Here β is the Prandtl factor and q is the dynamic pressure. The equivalent body of revolution due to lift thus corresponds to a body of revolution that begins at infinity with a finite base area (downstream or upstream). This equivalent body begins and ends where the lift starts and ends.

Minimum Drag Bodies

The wave drag for a body of revolution of given volume and length will be a minimum if its area distribution is that of Sears[17] and Haack[18] (corrected by Sears). Thus, for minimum wave drag due to volume we need a wing with a Sears–Haack area distribution in each azimuthal plane. As Smith observed,[6] this is the product of elliptic and parabolic distributions. The wave drag of a body of revolution with a given length and base area (corresponding to $2\beta/q$ times the lift) will be minimum if the area distribution is elliptical, that is, a Kármán ogive[19] (see also Sears[17]). An ellipse has the property that all chord distributions are elliptical. Thus, an oblique wing with an elliptical spanwise lift distribution will correspond to a Kármán ogive in each azimuthal plane. This spanwise elliptic load projects to an elliptic load in the vertical plane and thus also minimizes the induced drag. An elliptic wing with wing bending, as depicted in Fig. 2, to achieve an elliptic load will have the minimum drag due to lift.

Rawdon et al.[9] observed that there may be an excess of volume in a realistic oblique wing transport. Thus, a Sears area distribution, which minimizes the wave drag due to caliber, may be more appropriate than a Sears–Haack body. A Sears body has $\frac{8}{9}$ the wave drag of a Sears–Haack body of the same caliber.

Numerical results for an oblique elliptic wing wihout lift, swept to 60 deg, and flying at $M_\infty = \sqrt{2}$ with symmetrical cross sections and a Sears–Haack area distribution are compared with those of linear theory in Fig. 3. These results indicate strong nonlinear effects for practical oblique wing transports. These effects are reduced if the sweep angle is increased. Although linear panel methods provide a guide as to what can be achieved by an oblique wing supersonic transport,[7,8] nonlinear design methods that recognize the transonic nature of the flow normal to the leading edge, i.e., the crossflow, are used here.

Supercritical Airfoils

At cruise conditions the flow over an oblique wing is that behind the nearly conical shock wave emanating from the leading

tip. The wing is swept so that the component of the flow normal to the wing's leading edge will be sufficiently subsonic that thick, supercritical airfoil sections should be used to create the wing. We choose a freestream Mach number of $\sqrt{2}$ and an initial sweep angle of 60 deg, retreating from the higher values used in previous studies. The normal component of the Mach number is 0.707; the spanwise component Mach number is 1.235.

Although the flow over this swept wing is supersonic, the crossflow plane equations appropriate for an infinite oblique wing, or for a conical flow, are mixed, being hyperbolic outside the bow shock wave and inside the local supersonic crossflow region, but elliptic elsewhere. Thus, the fictitious gas method of Sobieczky et al.[20] for the design of supercritical airfoils was used to design the wing's airfoil sections. That this method may be applied to supersonic flows was first established by Sritharan.[21]

For the fictitious equations used in the Euler solver to suggest supercritical crossflow airfoils, we prescribed a new energy equation to change the crossflow equations inside the local supersonic region so that they remain elliptic-like there.[22] This results in a flow with a smooth sonic line, but the wrong gas law, inside the supersonic region. The correct mixed-type structure of the transonic flow is recovered in the next step: supersonic flow recalculation by means of the method of characteristics, using the just-calculated data on the sonic line for the initial values. This recomputation of the flow with the correct equations of state has a lower density in the supersonic flow and provides a modified, and only slightly thinner, airfoil design.

Geometry Generation

Aircraft wings are primarily designed on the basis of a planform shape and airfoil data for wing sections. Airfoil curvature modifications rather than thickness reductions are needed to provide shock-free transonic airfoils. This knowledge and aerodynamic knowledge base of the supporting theories just mentioned have led to geometry tools that provide the parameterized baseline configuration used here. A recent review of these tools and their applications may be found in Ref. 23.

Airfoil Sections

Figure 4 illustrates a spanwise element of an arbitrary wing. The geometrical properties are dominated by the wing section at a given span location. A set of support airfoils are blended to define wing sections at any span location. Requirements for an oblique wing transport, like control of the spanwise volume (wing section area) distribution and certain flow phenomena observed in earlier numerical modeling, suggest the need for special mathematical functions to define airfoil shapes of practical interest. These shapes are controlled by a small set of parameters whose selection is guided by a knowledge of transonic flow phenomena. This leads to the small number of parameters needed to effectively influence the flow structure and thereby the aerodynamic performance of the resulting airfoils.

Figure 5 shows the selected airfoil function with input of 11 basic geometric parameters. These parameters, $\boldsymbol{p}$, define the coefficients

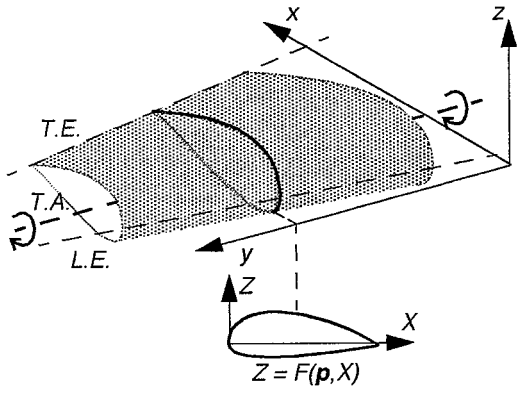

Fig. 4 Wing surface definition is by planform shape and by the spanwise airfoil and twist distributions. The airfoil shape is defined by the vector *p*.

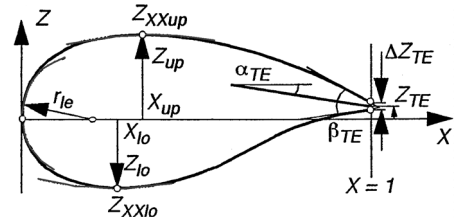

Fig. 5 The airfoil geometry is defined by 11 parameters: leading-edge radius; upper and lower crest locations and curvatures; trailing-edge ordinate, thickness and wedge angle.

of polynomials for upper and lower airfoil contours. Thus, the airfoil of Fig. 5 is prescribed by

$$Z = \sum_{n=1}^{6} a_n(\boldsymbol{p}) \cdot X^{n-\frac{1}{2}}$$

Most classical, as well as more sophisticated airfoils, are represented by this function with good accuracy.

The next step in defining the wing is the blending of the 11 airfoil parameters along the span by the same set of basic functions used to define piecewise any arbitrarily complex curve in a three-dimensional space. In this manual optimization only simple variations to the previously designed shock-free airfoil were considered. Most parameter variations are basically linear along the span, some of them are kept constant, but several parameters are modeled by curves. These are explained further here because of their importance in meeting the requirements prescribed by the aerodynamic theory. Visualization of the flowfield may further guide optimization as discussed in Refs. 24 and 25.

Planform and Wing Twist Axis

The basic wing shape is chosen to have an elliptic chord distribution while providing additional sweep back of the trailing portion of the wing. The twist axis is chosen to be the classical quarter chord location; its vertical coordinate z_{twist} defines dihedral or bending of the wing. Ellipses and parabolas are used here, requiring only a few data to define function values at any span station.

Thickness

The area of each airfoil section, with the airfoils generated using the 11 input parameters, is determined by integrating the polynomials for the upper and lower surfaces. The thickness is distributed to approximate a Sears–Haack body. For an elliptic planform and a constant baseline airfoil the vertical coordinate would be multiplied by an elliptic thickness distribution, and the resulting physical thickness distribution is parabolic.

Twist Distribution

A sensitive tool for the control of spanwise aerodynamic load distribution is local section twist. Parabolic wing bending z_{twist} provides most of the desired elliptic aerodynamic load. A nonlinear twist distribution along the trailing portion of the wing allows us to fine tune the lift distribution.

Curvature Parameters

The nose radius r_{le} and crest curvatures $Z_{xx,\text{up}}$ and $Z_{xx,\text{lo}}$ are useful in systematic design methods for supercritical transonic airfoils and wings. Earlier studies using a single shock-free airfoil in subsonic flow led to the observation that a single airfoil was not enough to generate an oblique wing with the pressure distribution needed for favorable viscous interaction. Thus, variation of the curvature parameters was necessary, and limited sensitivity studies were carried out. With the airfoil parameters given as functions of span and the spanwise wing sections prescribed by a polynomial, the height of any point on the wing above the plane of the wing can be determined rapidly without iteration and interpolation; this accelerates the optimization procedure considerably.

Results

Our design studies use the Euler algorithm of the code CFL3D developed by Thomas et al.[26] at NASA Langley. We used the O-O grid topology shown in Fig. 6. The geometry generator used a shock-free airfoil for the center section and then blended varying airfoil sections along a conventional ellipse planform with a 10:1 axis ratio. In our early studies we used twist to achieve an elliptic load distribution, and we only endeavored to minimize the drag due to lift, accepting the resulting wave drag due to volume caused by an elliptic (rather than parabolic) thickness distribution (see Ref. 27). This resulted in relatively strong crossflow shock formation on the wing's trailing tip and an unsatisfactory lift-to-drag ratio.

The center section thickness achieved with our supercritical airfoil designs was 19%. If the wing's centerline chord is 55 ft, the maximum center cabin height is 10.45 ft. The spanwise airfoil area and thickness factor distribution was chosen to provide a Sears–Haack area distribution as this ensured a maximum wing thickness of at least 7 ft over three-quarters of the wing's span. The geometric studies of Ref. 9 indicate that this wing should be able to seat 800 passengers.

A careful, manual selection of an asymmetrical planform with an elliptic chord distribution, approximate parabolic bending of the wing, and a nonlinear twist distribution were used to achieve a nearly elliptic load distribution. A straight quarter chord line (twist axis) in the leading portion of the wing plane was maintained, but an elliptic shape for its trailing portion was chosen to increase the sweep of this portion of the wing. The resulting parametric variations, including wing bending and the analytical variation of the set of generating parameters, are depicted in Fig. 7.

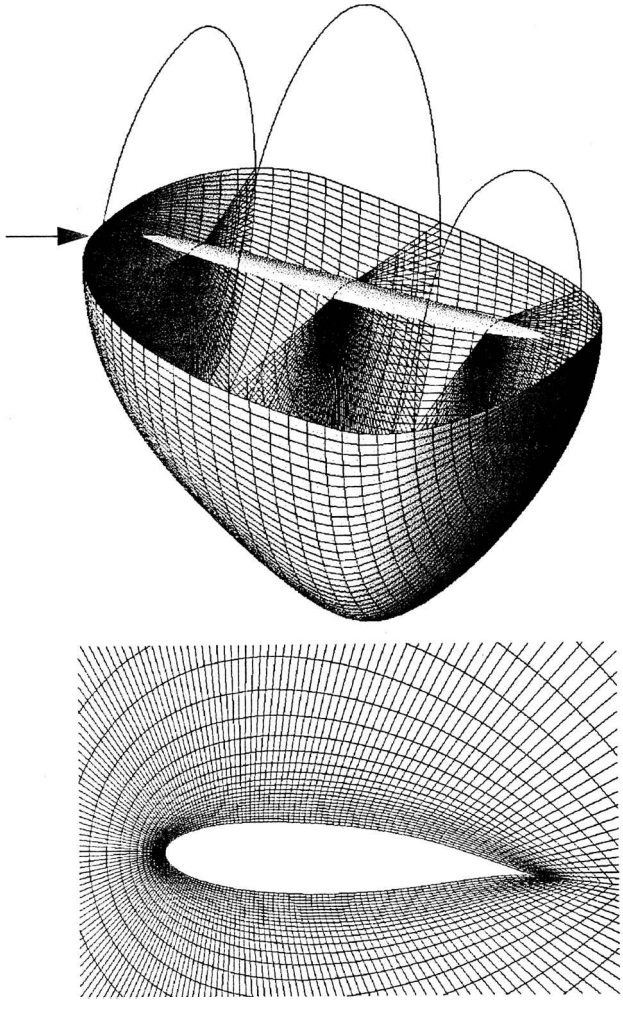

Fig. 6 The computational grid used in these studies had 193 × 41 × 33 grid points: around the sections; spanwise; and outward for each section.

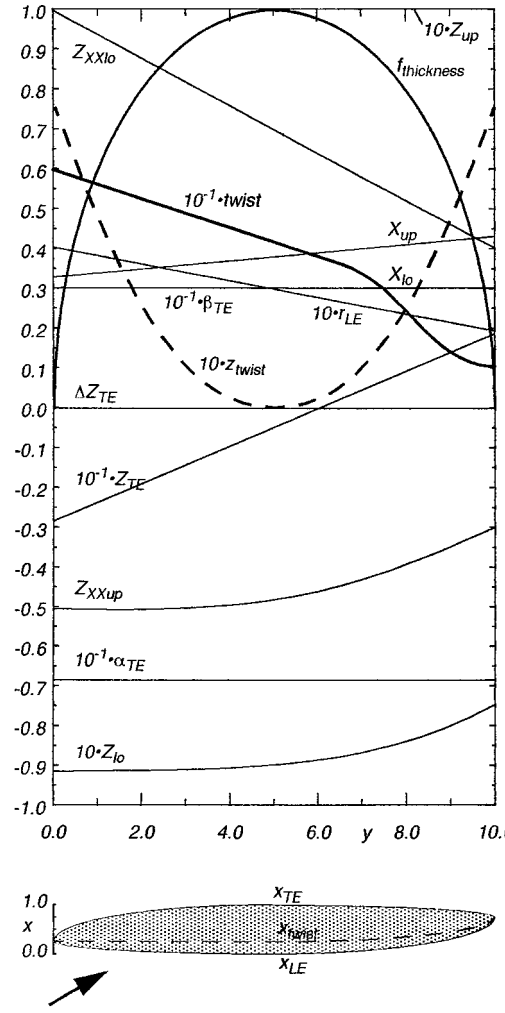

Fig. 7 Variation of airfoil design parameters and planform functions along the wing's span for the designed wing.

This manual optimization provides the inviscid analysis shown in Fig. 8. A supercritical crossflow pressure distribution is obtained with only moderate crossflow shocks. In a refined analysis of the flowfield with visualization tools, the crossflow shocks are identified as part of the trailing shock cone reaching upstream to the wing surface.[25] This suggests that the complete removal of the crossflow shocks on the surface is unlikely and reminds us of past efforts to find shock-free airfoils at too high transonic Mach numbers with inverse methods where hanging shocks persist in the flowfield even though the flow is shock-free at the airfoil surface. The wave drag of our oblique wing is dominated by the global influence of the area and load distributions. Controlling the crossflow shock strength is nevertheless necessary to prevent boundary-layer separation.

The inviscid L/D of this wing at the design condition is 21.3 at a C_L of 0.145. We then examined the effect of C_L at 60 deg of sweep on the inviscid L/D, as shown in Fig. 9a. L/D increases slightly to 21.6 as C_L is decreased to 0.125. We then examined the effects of sweep with C_L fixed at 0.135 as shown in Fig. 9b. With the sweep increased to 68 deg, the inviscid L/D increases to 26.3. Next we explored the effect of C_L with the sweep fixed at 68 deg, as shown in Fig. 9c. Lower lift coefficients provide marked increases in L/D. With $C_L = 0.0677$ we find a maximum inviscid L/D of 35.0. The dramatic improvement achieved with increased sweep should not be surprising. With higher sweep the wing is effectively thinner, and with its C_L lower linear theory is more applicable. This then corresponds to a manually optimized nonlinear, but inviscid, design that comes close to providing linear theory results. The viscous optimization then allows a further reduction in sweep for this optimum wing.

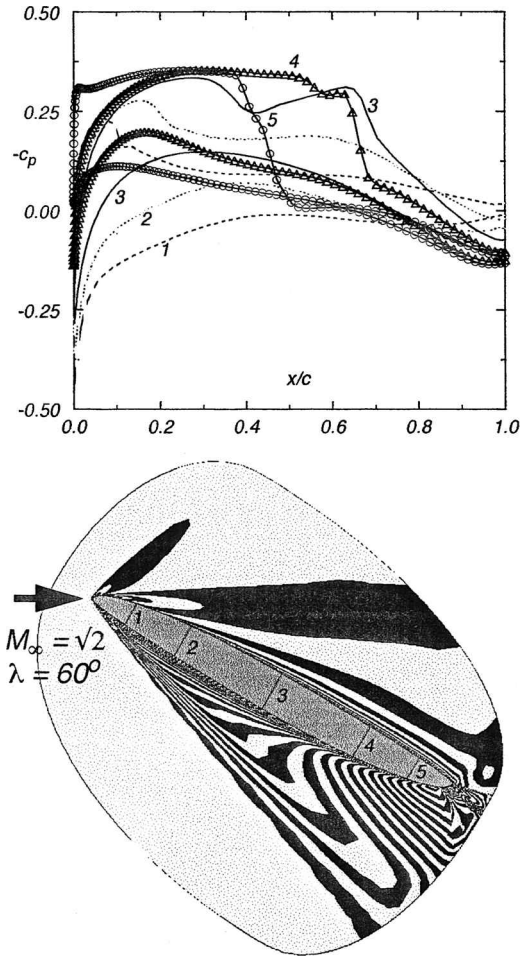

Fig. 8 Pressure distributions in the plane normal to the wing quarter chord and the corresponding isotach variations are shown for $M_\infty = \sqrt{2}$ with a sweep angle λ of 60 deg.

Viscous Optimization

As noted earlier, the design studies of Rawdon et al.,[9] as well as our own studies,[11,22] suggest that an oblique wing might require a maximum thickness of 10.5 ft and a maximum chord of 55 ft (19% thick). Low induced drag and wave drag are obtained with a 10:1 axis ratio planform, which results in a 550-ft wing span. This gives a planform area S of 23,758 ft^2 and a volume of 124,140 ft.^{3} Such an aircraft should accommodate 800 passengers. The studies of Rawdon et al.[9] suggest to us an estimated takeoff weight of 1.575 million lb, a weight upon entering cruise of 1.5 million lb, a weight upon leaving cruise of 0.9 million lb and a midcruise weight of 1.2 million lb.

This oblique wing supersonic transport will fly at the altitude that, considering viscous effects, maximizes L/D. Thus, when viscous effects are considered, we may improve L/D by increasing C_L and incurring a lower inviscid L/D, but thereby flying higher and reducing skin-friction drag. We may approximate the viscous drag as $2qSC_F$, where C_F is the wing average skin-friction coefficient for the wing's planform area at a Reynolds number Re based on the mean streamwise chord. The lift is qSC_L, and so we may write for our wing that

$$\text{Drag} = \text{Lift}[(D/L)_{\text{inviscid}} + 2C_F/C_L]$$

The drag on this wing is probably best approximated by using the method of Sommer and Short[28] as delineated by Peterson.[29] This method provides the Concorde's drag within a few percent.[30] We only used Navier–Stokes calculations to verify that the boundary layer did not appear to separate.

Figure 9c provides L/D as a function of C_L at a sweep of 68 deg. Given C_L, we can find what altitude gives maximum (viscous) L/D.

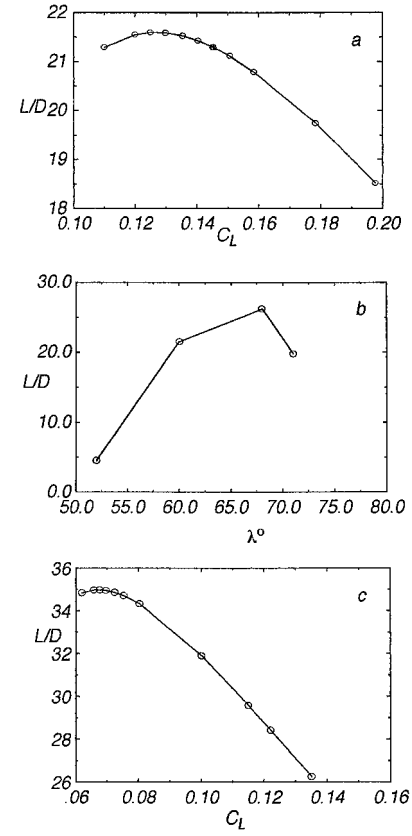

Fig. 9 Inviscid lift-to-drag ratios for the manually optimized design a) as a function of lift coefficient at fixed sweep, b) as a function of sweep at fixed lift coefficient, and c) as a function of lift coefficient at a preliminary determination of the optimum sweep.

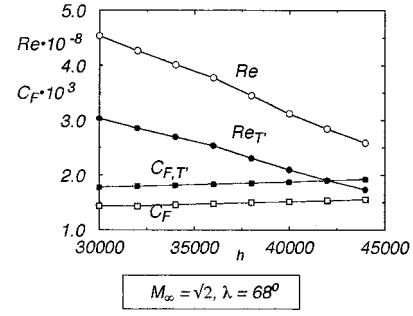

Fig. 10 Flight Reynolds number: the Reynolds number based on the reference temperature T' and the corresponding mean skin-friction coefficients, as a function of flight altitude for the conditions shown.

To do so, we must first provide the appropriate Reynolds numbers and determine the variation of C_F as a function of flight altitude. We assume the wall is adiabatic and use the planform area as the area of the two-sided flat plate for which we compute the viscous drag (this area may thus be low by 2–3%). The streamwise chord is the mean chord divided by cos λ. The appropriate reference temperature T' for the boundary layer is determined from Ref. 29. Figure 10 provides $C_{F,T'}$ as a function of the altitude h. The C_F we would have found if we had used the freestream Reynolds numbers is also shown. Given C_L and a weight upon entering cruise of 1.5 million lb, we can then construct Fig. 11 to find that the drag-to-lift ratio is a minimum at $C_L = 0.1221$.

We use our inviscid analysis of the flow under these conditions to find that

$$\left(\frac{L}{D}\right)_{\text{opt}} = \left[\frac{1}{28.423} + 2\left(\frac{0.001523}{0.1221}\right)\right]^{-1} = 16.6$$

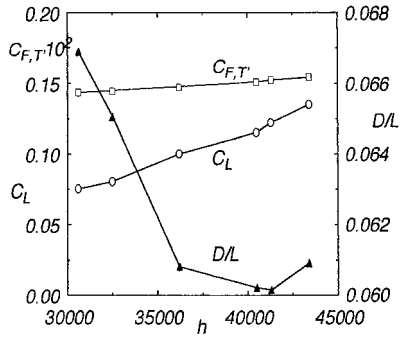

Fig. 11 Lift coefficient, skin-friction coefficient, and drag-to-lift ratio as a function of flight altitude.

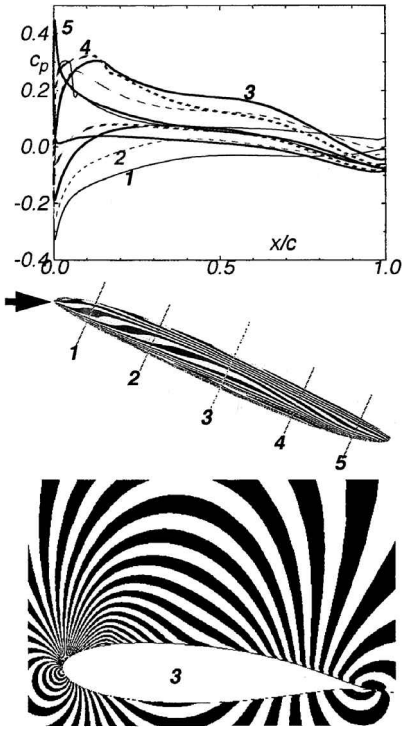

Fig. 12 Pressure distributions in the plane normal to the wing quarter chord and the corresponding isotach variations are shown for $M_\infty = \sqrt{2}$ with a sweep angle λ of 65 deg.

which corresponds to $ML/D = 23.5$. Given the flight altitude of 41,300 ft and C_F, the viscous drag is determined to be 37,420 lb. We have reduced inviscid L/D from its maximum of 34.96 to 28.42 by increasing C_L so we may fly higher. Although C_F increases slightly with altitude, the dynamic pressure and thereby skin-friction drag, are reduced significantly, thereby improving L/D. No doubt formal mathematical methods such as the self-adjoint method of Jameson[31] applied with the geometry generator used here could further improve this result.

Optimum Sweep

We then reconsidered the effect of sweep and Mach number on L/D and ML/D. With $M_\infty = \sqrt{2}$ a sweep of 65 deg gave an optimum inviscid L/D of 30.29 and a corresponding ML/D of 42.8. An increase in M_∞ to 1.5 resulted in a decrease in ML/D to 39.4. From this we conclude that the best cruise conditions for this manually optimized wing are with $M_\infty = \sqrt{2}$, $\lambda = 65$ deg, and $C_L = 0.1221$. This reduces the streamwise chord of the wing and increases the average skin-friction coefficient to 0.001558, resulting in an optimum viscous lift-to-drag ratio:

$$\left(\frac{L}{D}\right)_{\text{opt}} = \left[\frac{1}{30.287} + 2\left(\frac{0.001558}{0.1221}\right)\right]^{-1} = 17.08$$

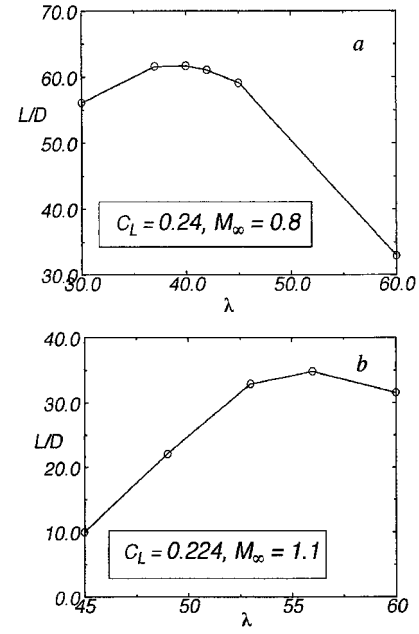

Fig. 13 Off-design lift-to-drag ratio as a function of sweep at fixed C_L and M_∞. The lift coefficients used correspond to those for acceleration to cruise.

with a corresponding ML/D of 24.2. Results for the inviscid flow analysis at $\lambda = 65$ deg are shown in Fig. 12.

Linear Theory *ML/D*

For these conditions (1.5 million lb; 41,300 ft; $\lambda = 65$ deg; $M_\infty = \sqrt{2}$) linear theory gives a drag due to lift of 28,980 lb and a drag due to volume of 16,450 lb, for an inviscid drag of 45,430 lb and an ideal inviscid L/D of 33.0. The viscous drag is 38,280 lb, and the linear theory drag plus skin-friction drag provide an optimum L/D of 17.9. Our manually optimized design achieved 17.1. If we had taken a Sears area distribution, the drag due to volume would be reduced by $\frac{8}{9}$; this would improve the linear theory L/D to 18.3 (including viscous drag).

During cruise, the aircraft climbs to maintain C_L as fuel is burned. For the midcruise weight of 1.2 million lb, the wing flies at 46,000 ft. At the end of cruise with a weight of 0.9 million lb, the wing flies at 52,000 ft.

Acceleration to Cruise

If our oblique wing weighs 1.575 million lb on takeoff, achieves $M_\infty = 0.8$ at 1.55 million lb, and $M_\infty = 1.1$ at 1.525 million lb (based on 5% of fuel to climb to cruise), it will enter cruise ($M_\infty = \sqrt{2}$) weighing 1.5 million lb. As the wing accelerates to cruise conditions, its Mach number and altitude are increasing. The wing's sweep that optimizes inviscid L/D is shown in Fig. 13 for an appropriate C_L. At Mach 0.8, with the wing flying at C_L of 0.24, the optimum sweep is 40 deg, and its flight altitude for 1.55 million lb is 30,800 ft. Under these conditions this wing achieves the astounding inviscid L/D of 61.7. The corresponding viscous L/D is 31.1, and the ML/D is 24.9. Because of its good transonic performance, the aircraft continues to climb to cruise altitude of 41,300 ft while it accelerates to $M_\infty = 1.1$.

At Mach number 1.1 we find the optimum sweep to be 56 deg. At a weight of 1.525 million lb, with Mach 1.1, the aircraft will fly at 41,300 ft with $C_L = 0.205$. At $C_L = 0.205$ the invisicid L/D is 35.0 with $\lambda = 56$ deg. This corresponds to viscous L/D of 21.5 and ML/D of 23.7. The oblique wing then accelerates in level flight to its cruise Mach number of $\sqrt{2}$ where the L/D is 17.1 and the ML/D is 24.2.

Conclusion

With linear theory as a guide, a large wing was manually optimized and attains an ML/D of 24.2 at the cruise Mach number of

$\sqrt{2}$ and an altitude of 41,300 ft. This compares well with the linear theory optimum of 25.3. Given the transonic nature of the crossflow, designs that exceed the linear theory optimum seem possible.

This result does not include trim drag. Contemporary control technology, as recently demonstrated in the X-36 program, suggests that trailing-edge control surfaces and vectored thrust would be used to provide pitch and yaw stability.

Because of good transonic performance, this oblique wing accelerates to $M_\infty = 0.8$ at 30,800 ft with its takeoff sweep of 40 deg. At these conditions its ML/D is 24.9. It continues to climb to 41,300 ft, increasing its sweep to 56 deg and accelerating to $M_\infty = 1.1$ where it has an ML/D of 23.7. It then accelerates in level flight, increasing its sweep to 65 deg, to cruise at $M_\infty = \sqrt{2}$ with an ML/D of 24.2.

The remarkable Concorde has an ML/D of about 15. The oblique wing aircraft, designed manually here, achieves 24.2. With vectored-thrust engines embedded in the wing, there is no need for vertical control surfaces. Thus, an oblique wing supersonic transport will have much higher cruise ML/D than the Concorde. This is also higher than we might expect from the next generation of subsonic transports, which, when large, may be symmetrical all-wing aircraft. This aircraft also has much better off-design performance than the Concorde and flies efficiently at $M_\infty = 1.1$. At this speed its sonic boom would be refracted and not reach the ground. Consequently, it could be operated over land at speeds 25–30% higher than those of current subsonic transports.

Acknowledgments

This work was funded by an Alexander von Humboldt Foundation Max Planck Research Prize, a NSF CISE Postdoctoral Research Associateship, and DLR basic research funding. Computer support was provided by NASA's Numerical Aerodynamic Simulator Program.

References

[1]Jones, R. T., "The Minimum Wave Drag of Thin Wings in Frictionless Flow," *Journal of the Aeronautical Sciences*, Vol. 18, No. 2, 1951, pp. 75–81.

[2]Jones, R. T., "Theoretical Determination of the Minimum Wave Drag of Airfoils at Supersonic Speeds," *Journal of the Aeronautical Sciences*, Vol. 19, No. 12, 1952, pp. 813–822.

[3]Hayes, W. D., "Linearized Supersonic Flow," North American Aviation, Rept. AL 222, Los Angeles, 1947 (reprinted as Princeton Univ. Aerospace and Mechanical Sciences Rept. 852).

[4]Lomax, H., "The Wave Drag of Arbitrary Configurations in Linearized Flow as Determined by Areas and Forces in Oblique Planes," NACA RM A55A18, 1955.

[5]Lomax, H., and Heaslet, M. B., "Recent Developments in the Theory of Wing-Body Wave Drag," *Journal of the Aeronautical Sciences*, Vol. 23, No. 12, 1956, pp. 1061–1074.

[6]Smith, J. H. B., "Lift/Drag Ratios of Optimized Slewed Elliptic Wings at Supersonic Speeds," *Aeronautical Quarterly*, Vol. 12, 1961, pp. 201–218.

[7]Van der Velden, A. J. M., "Aerodynamic Design of the Oblique Flying Wing Supersonic Transport," Ph.D. Dissertation, Dept. of Aeronautics and Astronautics, Stanford Univ., Palo Alto, CA, SUDAAR 621, June 1992.

[8]Van der Velden, A. J. M., "The Oblique Flying Wing Transport," *New Design Concepts for High Speed Transport*, edited by H. Sobieczky, CISM Courses and Lectures Vol. 366, Springer–Verlag, Vienna/New York, 1997, pp. 291–315.

[9]Rawdon, B. K., Scott, P. W., Liebeck, R. H., Page, M. A., Bird, R. S., and Wechsler, J., "Oblique All-Wing SST Concept," McDonnell Douglas CR, NAS1-19345, 1994.

[10]Galloway, T., Gelhausen, P., Moore, M., and Waters, M., "Oblique Wing Supersonic Transport," AIAA Paper 92-4230, Aug. 1992.

[11]Li, P., Seebass, R., and Sobieczky, H., "The Oblique Flying Wing as the New Large Aircraft," *Proceedings of the 20th International Council of the Aeronautical Sciences Congress*, 96.4.4.2, 1996, pp. 1–10.

[12]Seebass, R., "Oblique Flying Wing Studies," *New Design Concepts for High Speed Transport*, edited by H. Sobieczky, CISM Courses and Lectures Vol. 366, Springer–Verlag, Vienna/New York, 1997, pp. 317–336.

[13]Cheung, S., "Viscous CFD Analysis and Optimization of an Oblique All-Wing Transport," NASA CDCR-20005, 1994.

[14]Munk, M., "The Reversal Theorem of Linearized Supersonic Airfoil Theory," *Journal of Applied Physics*, Vol. 21, Feb. 1950, pp. 159–160.

[15]Kogan, M. N., "On Bodies of Minimum Drag in a Supersonic Gas Flow," *Prikladnaya Matematika y Mekanika*, Vol. 21, No. 2, 1957, pp. 207–212.

[16]Jones, R. T., "The Minimum Wave Drag of Thin Wings at Supersonic Speeds According to Kogan's Theory," *Theoretical and Computational Fluid Dynamics*, Vol. 1, 1989, pp. 97–103.

[17]Sears, W. R., "On Projectiles of Minimum Wave Drag," *Quarterly of Applied Mathematics*, Vol. 4, No. 4, 1947, pp. 361–366.

[18]Haack, W., "Geschossformen Kleinsten Wellenwiderstandes," *Lilienthal-Gesellschaft für Luftfahrt*, Rept. 139, 1941, pp. 14–28.

[19]von Kármán, Th., and Moore, N. B., "Resistance of Slender Bodies Moving with Supersonic Velocities with Special Reference to Projectiles," *Transaction of the American Society of Mechanical Engineers*, Vol. 34, 1932, pp. 303–310.

[20]Sobieczky, H., Fung, K.-Y., Seebass, A. R., and Yu, N. J., "New Method for Designing Shock-Free Transonic Configurations," *AIAA Journal*, Vol. 17, No. 7, 1979, pp. 722–729.

[21]Sritharan, S. S., "Delta Wings with Shock-Free Cross Flow," *Quarterly of Applied Mathematics*, Vol. 43, No. 3, 1985, pp. 275–286.

[22]Li, P., Sobieczky, H., and Seebass, A. R., "A New Design Method for Supersonic Transport," AIAA CP 95-1819, 1995.

[23]Sobieczky, H., "Geometry Generator for CFD and Applied Aerodynamics," *New Design Concepts for High Speed Transport*, edited by H. Sobieczky, CISM Courses and Lectures Vol. 366, Springer–Verlag, Vienna/New York, 1997, pp. 137–158.

[24]Hannemann, M., and Sobieczky, H., "Visualization of High Speed Aerodynamic Configuration Design," *Proceedings Visualization 95*, edited by D. Silver, Inst. of Electrical and Electronics Engineers, Computer Society Press, Los Alamitos, CA, 1995, pp. 355–358.

[25]Sobieczky, H., Seebass, R., Li, P., and Hannemann, M., "Manual Optimization of Oblique Flying Wing," *Proceedings of the 21st International Council of the Aeronautical Sciences Congress*, International Council of the Aeronautical Sciences, ICAS-98-2,1,3, 1998, pp. 1–11.

[26]Thomas, J. L., Taylor, S. L., and Anderson, W. K., "Navier–Stokes Computations of Vortical Flows over Low Aspect Ratio Wings," *AIAA Journal*, Vol. 28, No. 2, 1990, pp. 205–212.

[27]Li, P., Seebass, R., and Sobieczky, H., "Oblique Flying Wing Aerodynamics," AIAA Paper 96-2120, June 1996.

[28]Sommer, S. C., and Short, B. J., "Free-Flight Measurements of Turbulent Boundary Layer Skin Friction in the Presence of Severe Aerodynamic Heating at Mach Numbers From 2.8 to 7.0," NACA TN 3391, 1955.

[29]Peterson, J. B., "A Comparison of Experimental and Theoretical Results for the Compressible Turbulent Boundary Layer Skin Friction with Zero Pressure Gradient," NASA TN-D 1795, 1963.

[30]Jobe, C. E., "Prediction and Verification of Aerodynamic Drag, Part I: Prediction," *Thrust and Drag: Its Prediction and Verification*, edited by E. E. Covert, Progress in Astronautics and Aeronautics, Vol. 98, AIAA, New York, 1985, pp. 121–171.

[31]Jameson, A., "Optimum Aerodynamic Design Using CFD and Control Theory," AIAA Paper 95-1729, June 1995.